Title

Pursuit of Record Breaking Energy Barriers: A Study of Magnetic Axiality in Diamide Ligated Dy^{III} Single-Molecule Magnets.

Journal

Journal of the American Chemical Society, 139(4)

ISSN

0002-7863

Authors

Harriman, Katie LM
Brosmer, Jonathan L
Ungur, Liviu
et al.

Publication Date

2017-02-01

DOI

10.1021/jacs.6b12374

Peer reviewed

In the Pursuit of Record Breaking Energy Barriers: A Study of Magnetic Axiality in Diamide Ligated Dy^{III} Single-Molecule Magnets

Katie L. M. Harriman,[1] Jonathan L. Brosmer,[2] Liviu Ungur,*[,3,4] Paula L. Diaconescu,*[,2] and Muralee Murugesu*[,1]

[1] Department of Chemistry and Biomolecular Sciences, University of Ottawa, Ottawa, Ontatio K1N 6N5, Canada

[2] Department of Chemistry and Biochemistry, University of California, Los Angeles, California 90095, USA

[3] Theory of Nanomaterials Group and INPAC – Institute of Nanoscale Physics and Chemistry, Katholieke, Universiteit Leuven, Celestijnenlaan 200F, 3001 Leuven, Belgium

[4] Theoretical Chemistry, Lund University, Getingevagen 60, 22100, Lund Sweden

Supporting Information Placeholder

ABSTRACT: Dy^{III} single-ion magnets (SIMs) with strong axial donors and weak equatorial ligands have recently been sought after as model systems with which to harness the maximum magnetic anisotropy of Dy^{III} ions. Utilizing a rigid ferrocene diamide ligand (NN^{TBS}), a Dy^{III} SIM, (NN^{TBS})DyI(THF)$_2$, **1-Dy** (NN^{TBS} = fc(NHSi*t*BuMe$_2$)$_2$, fc = 1,1' ferrocenediyl), composed of a near linear arrangement of donor atoms, exhibits a large energy barrier to spin reversal (770.8 K) and magnetic blocking (14 K). The effects of the transverse ligands on the magnetic and electronic structure of **1-Dy** were investigated through *ab initio* methods, eliciting significant magnetic axiality, even in the 4th Kramers doublet, thus, demonstrating the potential of rigid diamide ligands in the design of new SIMs with defined magnetic axiality.

Magnetic anisotropy is arguably the most influential parameter that determines the performance of a lanthanide single-molecule magnet (SMM). Being able to design molecular species with defined magnetic axiality has allowed chemists to produce molecules possessing large energy barriers to spin reversal (U_{eff}) and, in some cases, magnetic blocking, reaching blocking temperatures (T_B) as high as 20 K.[1] In that regard, those SMMs containing only a single metal center, single-ion magnets (SIMs), have recently garnered significant interest in the field of molecular magnetism, as the observed magnetic properties exist in the absence of magnetic exchange interactions, meaning that the experimentally determined performance of SIMs must arise from the combination of unquenched orbital angular momentum and crystal field contributions. This allows a tailored synthetic approach, which in recent years has evolved to include high symmetry crystal fields,[1-3] the introduction of main group ligands,[4] and the implementation of bulky ligands to obtain low coordination numbers.[5,6] However, the common theme among all of these systems is the devotion to harnessing the maximum magnetic anisotropy from the metal ion, especially if the metal is a lanthanide. The inherent magnetic anisotropy of *4f* ions results from the combination of large magnetic moments and spin-orbit coupling, where contributions from the crystal field can significantly enhance the magnetic anisotropy of a lanthanide SIM. In this respect, recent reports have focused on generating design criteria with which to elicit strictly axial anisotropy.[7,8] In particular, the motivation for the current study presented itself from our previous investigation of a series of dinuclear lanthanide SMMs.[9] This work utilized a rigid ferrocene diamide framework to support an inverse sandwich compound, exhibiting unprecedented uniaxial anisotropy, aligned with the shortest Dy-N bond.[9] Thus, by removing the central bridging moiety, the crystal field imposed by the amide groups may enhance the SMM properties, since linearly coordinated negatively charged donor atoms may result in harnessing the maximum angular momentum originating from the Dy^{III} ion. This unique class of diamide ligands parallels the structural features of the diketiminates that have been popular in the fields of molecular magnetism, catalysis, and bioinorganic chemistry.[10,11] However, the ferrocene diamides have the ability to produce a wider bite angle, while still maintaining the rigidity of the backbone. This is an attractive feature if we wish to approach linearity and effectively mimic two-coordinate Dy^{III} compounds, which still remain a synthetic challenge. Thus, these designer ligands represent a promising alternative to generating pseudo-axiality in Dy^{III} compounds. To this end, we discuss the properties of (NN^{TBS})DyI(THF)$_2$, **1-Dy** (NN^{TBS} = fc(NHSi*t*BuMe$_2$)$_2$, fc = 1,1′ ferrocenediyl, Figure 1), which provides a unique design approach toward Dy^{III} molecules with defined magnetic axiality.

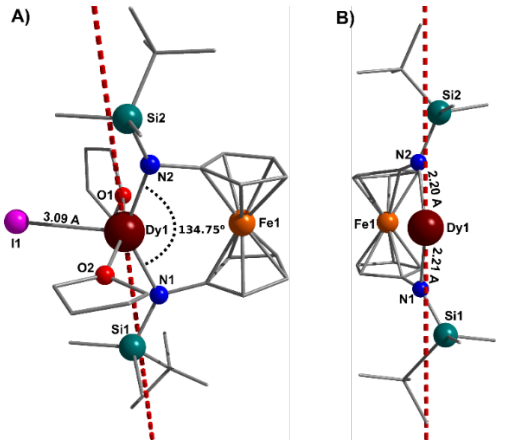

Figure 1. Structural representation of (a) **1-Dy** and (b) NN^{TBS} ligand metal bonding. Dashed lines represent the main magnetic axis in the ground, first excited, and second excited Kramers doublet states (states ±1, ±2 and ±3 in Figure 3).

The single crystal X-ray diffraction structure of **1-Dy** was previously reported,[9] but, for clarity purposes, it will be discussed herein. Complex **1-Dy** crystallizes in the triclinic space group *P*-1. Each asymmetric unit contains one Dy^{III} ion coordinated to one NN^{TBS} ligand through two nitrogen donor atoms that effectively produce a bite angle of 134.7(2)° (Figure 1a). The coordination sphere of the Dy^{III} ion is completed by two molecules of THF and an iodide ligand. The exact geometry of this five-coordinated Dy^{III} was confirmed *via* SHAPE analysis, producing results most consistent with a trigonal pyramid geometry of D_{3h} symmetry (Table S1).[12] Interestingly, short Dy-N distances of 2.21(2) and 2.20(6) Å are observed (Figure 1b), with only seven reported examples with Dy-N distances shorter or equal to 2.20 Å.[13-17] The observed Dy-N distances of **1-Dy** are smaller than the sum of the ionic radii (2.62 Å),[18] suggesting that a dominant electrostatic interaction exists between the nitrogen atoms of the NN^{TBS} ligand and the Dy^{III} ion. However, covalent contributions to the bonding cannot be dismissed. The presence of such strong interactions in the axial positions of this Kramers ion has the ability to harness significant magnetic anisotropy, through taking advantage of its oblate electron density.[19] Thus, theoretically, significant T_B and U_{eff} values may be expected to arise from this type of bonding interaction in **1-Dy**. Nonetheless, within the lattice, these molecules are well separated, producing a minimum Dy^{III}–Dy^{III} distance of 9.776(5) Å (see Figure S1 for crystallographic packing). While direct and superexchange pathways have been considered negligible at this distance, intermolecular dipolar interactions remain a possibility (*vide infra*). At such a scale, slower relaxation processes have been attributed to dipolar mediated relaxations in 5*f* single-ion systems.[20] Collectively, the presence of strong metal-ligand interactions through the nitrogen atoms of the NN^{TBS} ligand and the well separated nature of paramagnetic centers within the lattice are expected to yield strong slow relaxation dynamics originating from the Dy^{III} ion (*vide infra*).

To investigate the consequence of this type of ligand architecture on the local anisotropy of the Dy^{III} ion, magnetic susceptibility measurements were performed using a SQUID magnetometer. Under an inert atmosphere, to prevent sample degradation, a ground polycrystalline sample was prepared with 30 mg of **1-Dy**. Direct current (dc) magnetic susceptibility measurements were performed in the temperature range 1.8 – 300 K, under a static field of 1000 Oe. At room temperature, the χT value of 13.99 cm^3Kmol^{-1} is in good agreement with the theoretical value of 14.17 cm^3Kmol^{-1} for a mononuclear Dy^{III} ($^6H_{15/2}$, $S = 5/2$, $L = 5$, $g = 4/3$) complex (Figure S2). The experimentally determined room temperature χT value is slightly smaller than the theoretical value, presumably due to the splitting of the $^6H_{15/2}$ ground state.[1] Upon cooling, the χT product remains relatively constant with only a slight decrease until 8 K, suggesting the presence of a well separated low-lying energy spectrum (*vide infra*). Below this temperature, the χT product rapidly drops, reaching a minimum value of 9.67 cm^3Kmol^{-1} at 1.8 K. The abrupt decrease in the χT profile is indicative of magnetic blocking, where the system cannot reach an equilibrated population distribution due to the energy barrier to spin reversal. This phenomenon has been observed in other highly anisotropic lanthanide-based systems.[1, 5, 21, 22] To complement this, the isotemperature magnetization curve at 1.9 K saturates at 5.28 μ_B mol^{-1}, further suggesting the well separated nature of the ground state (Figure S3). Large separations between the ground state and excited states are highly sought after as it remains the origin for large spin reversal barriers, a necessary feature for the future incorporation of SMMs into technological devices. This finding is also in accordance with the *ab initio* determined energy of the first excited Kramers doublet which possess an energy of 414.6 cm^{-1} (*vide infra*); which is one of the largest separations observed between the ground state and excited states in any Dy^{III} SMMs.[1, 5, 21, 22] This large separation ensures that thermal relaxation will at least occur *via* this energy, yielding an impressive barrier to the slow relaxation of the magnetization.

The presence of magnetic blocking, as evidenced from the characteristic low temperature profile of the χT curve (i.e., plummeting of the χT product below 8 K), was probed with magnetic hysteresis measurements in the range of 50 to -50 kOe, at an average sweep rate of 23 Oe s^{-1} (Figure S4). The complex displays clear hysteretic behavior at 1.9 K at $H = 0$ Oe. Upon raising the temperature, openings at $H = 0$ Oe are observed up until 5 K, and at $H \neq 0$ Oe openings can be observed up to 14 K at higher magnetic fields. Comparatively, the abrupt drop in the χT product at 8 K also serves as a reference in terms of magnetic blocking. However, the discrepancy between these observed values may result as a consequence of mixed relaxation processes, specifically Raman and direct relaxation processes that occur at low temperature.[5] The possibility of mixed relaxation mechanisms cannot be discarded given the low temperature data of the frequency dependent susceptibility (Figure 3). Lastly, the possibility of mixed relaxation mechanisms is further supported by the distribution of relaxation times obtained from the dynamic susceptibility data (see below for discussion and Tables S2-S3).

Alternating current (ac) magnetic susceptibility measurements were performed to probe the possibility of multiple relaxation processes. Within the range 0.1-1500 Hz, a single peak in the out-of-phase (χ") susceptibility was observed between 1.9 and 60 K, with shifting peak maxima toward lower frequency (Figure 2 and S5). The relaxation time was extracted for each isotemperature curve of the in-phase (χ') and χ" susceptibilities *via* the generalized Debye model.[23] A narrow distribution of relaxation times was found for the entire data set,

yielding an α parameter of ≤ 0.17 (Tables S2 and S3). Comparatively, relaxation times obtained from fitting the Cole-Cole plot (Figure S6) to the generalized Debye model produced similar results (α ≤ 0.22), with only a single deviation occurring for the 6 K curve, resulting in α = 0.50.

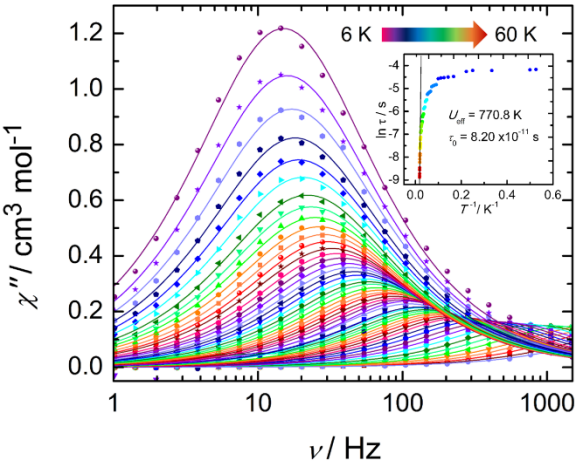

Figure 2. Frequency dependence of the χ'' magnetic susceptibility for **1-Dy** under zero applied dc field from 6 K to 60 K (for data below 6 K see Figure S5). Solid lines represent best fits to the generalized Debye model. *Inset:* Relaxation time of the magnetization, $ln(\tau)$ *vs.* T^{-1}; the solid black line corresponds to the linear fit to the Arrhenius equation.

The zero-field χ'' data was fit to the Arrhenius law ($\tau = \tau_0 \exp[U_{eff}/(k_B T)]$) to give an energy barrier to spin reversal of 770.8 K (535.7 cm^{-1}) and a pre-exponential factor of 8.20 x 10^{-11} s. An energy barrier of this magnitude is rare in lanthanide based systems as they are often plagued with significant ground state tunneling arising from their classically dense energy spectra.[24] Such that, there exists only two reports of monometallic dysprosium compounds exhibiting larger barriers.[5, 21] In the case of **1-Dy**, the extracted energy barrier of 770.8 K is in good agreement with the computationally determined thermally activated relaxation process through the third and fourth KDs (Figure 3). The plot of the natural log of the relaxation time *versus* reciprocal temperature remains linear in the high temperature regime (Figure 2 *inset*). This feature strongly correlates to a dominant thermally activated Orbach relaxation regime.[25] The plot remains linear until 26 K, when it experiences a deviation from the Arrhenius law. Which is easily visualized through the overlapping peak maxima at lower frequencies in the χ'' susceptibility (Figure 2). The observed behavior may arise from mixed relaxation mechanisms, although it is likely dominated by quantum tunneling of the magnetization (QTM).

To suppress any contribution of QTM to the obtained spin reversal barrier, frequency dependent measurements were carried out under various static fields (0-1200 Oe) (Figure S7). At fields smaller than 100 Oe, a single peak was observed in the χ'' susceptibility, however, when collected at 100 Oe, a broad shoulder at low frequencies becomes evident, which has been previously observed at small fields in other Dy^{III} SIMs.[26] This process is augmented by increased static fields, until 400 Oe, where both processes are unobservable. An Argand plot was utilized in order to abstract the relaxation time of each *iso*-field curve *via* the generalized Debye model (Figure S8), providing a distribution of relaxation times with 0.89 ≥ α ≥ 0.25 (Table S5). Selection of a small optimal dc field of 150 Oe was utilized in order to probe the relaxation dynamics of the secondary process. Under these conditions a single peak in the frequency dependent χ'' susceptibility was observed between 54 K and 1.9 K (Figures S9 and S10). Similar to the zero-field ac susceptibility, this process's frequency dependence is arrested below 16 K. Fitting the data to the Arrhenius laws yields an energy barrier to spin reversal of 348.9 K (242.5 cm^{-1}) and a pre-exponential factor of 3.27 x 10^{-7} s (Figure S11). Fitting this process to the generalized Debye model *via* an Argand plot (Figure S12) revealed a distribution in the relaxation times to give 0.011 ≤ α ≤ 0.404 (Table S6). The presence of the secondary process becomes evident as a shoulder/broad signal at 16 K, and emerges as an independent peak at 4 K. From the collected data, it is difficult to conclude the nature of the secondary process.

Ab initio calculations for **1-Dy** were performed in order to gain additional insight into the electronic and magnetic structure of this compound and to analyze the factors that contribute to lowering the magnetization blocking barrier. All calculations were of the CASSCF/RASSI/SINGLE_ANISO kind using the MOLCAS-8.0 program package,[27] details are provided in the Supporting Information. Properties of the investigated molecule were calculated on the basis of the computer spin-orbit states. A comparison of measured and calculated magnetic susceptibilities is given in Figure S2. Using previously proposed methodology, the magnetization-blocking barrier for **1-Dy** was calculated (Figure 3).[28, 29] From the obtained *ab initio* results, the parameters of the effective crystal-field Hamiltonian were extracted (Table S8). Analysis of the magnetization blocking barrier (Figure 3), provides a transverse magnetic moment of 1.5x10^{-4} μ_B, providing evidence for reduced QTM in the ground state of **1-Dy**, thereby permitting the observation of the zero filed SMM behavior (*vide supra*). Similarly, tunneling through thermally activated m_j = ±13/2 is also minimized, this is due in part to the co-linearity of the anisotropic axes of the ground and first excited state (*see* Figure 1). These findings correlate strongly with the obtained *g*-tensors, demonstrating significant magnetic axiality even at the m_j = ±11/2 states (*vide infra*). Based on the transverse magnetic moments (indicated above the arrows in Figure 3), the most probable pathway (red arrows) for magnetic relaxation encompasses the third and fourth KDs, while the experimentally obtained energy barrier lies only marginally below the third KD. Thus, the presence of mixed relaxation mechanisms may contribute to the lowering of the experimental energy barrier from the anticipated energy of the third KD. This is not surprising, given the experimental ac magnetic susceptibility behavior of **1-Dy** under zero field and 150 Oe (*vide supra*). Notably, the magnetic moment of an Orbach relaxation (green arrows) from m_j = -13/2 to m_j = +9/2 is only narrowly smaller than the tunneling between m_j = ±11/2 states (4.2 x 10^{-1} μ_B *vs.* 4.5 x 10^{-1} μ_B), suggesting that a competition between these two pathways may also contribute to the lowering of the experimental barrier.

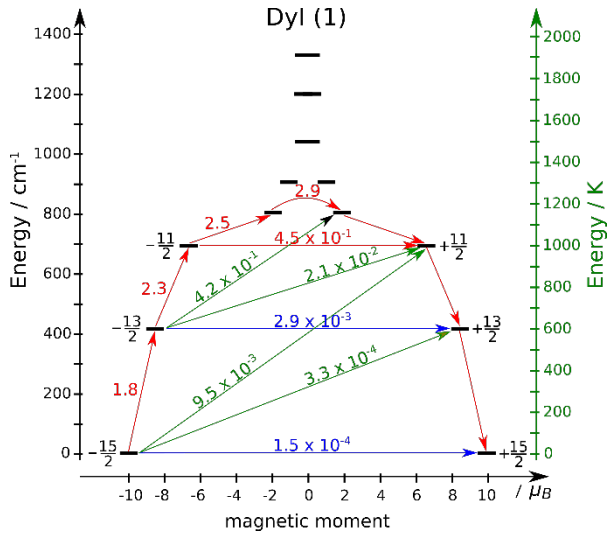

Figure 3. Magnetization blocking barrier of **1-Dy**. Arrows depict the most probable path for magnetic relaxation (red), QTM (blue), and Orbach relaxation (green).

It is important to mention that *ab initio* results are not based on direct fitting of the experimental data (in contrast to various phenomenological models).[30, 31] The methods may be straightforwardly applied for the investigation of molecules prior to their synthesis or for the evaluation of molecular properties upon various distortions employed. In this respect, we have developed and analyzed three different models in addition to **1-Dy**, in order to see the effects of THF and iodide ligands on the electronic and magnetic properties of the title molecule. Three models have been prepared: **1-noTHF** – containing no THF ligands, **1-noI** – containing no iodide ligand and **1-noTHFnoI**– where THF and iodide ligands were removed from the molecular structure. These models systematically remove the transverse ligands, allowing for a direct study of the ligand field effects which originate in **1-Dy**. In understanding the factors which contribute to lowering the experimental energy barrier we can then find improved ways for augmenting the local magnetic axiality in other low coordinate Dy^{III} systems. By employing similar CASSCF/RASSI/SINGLE_ANISO calculations with exactly the same computational options as employed for the original compound **1-Dy**, the energy splitting of the ground free ion $J = 15/2$ was obtained for all models and the title compound, see Table S9.

Analysis of the low-lying energy spectra of the abovementioned models and the title compound reveals a strong increase in the splitting of the ground free ion $J = 15/2$ when THF ligands are removed, **1-noTHF**, as well as when the iodine ligand is removed, **1-noI**. With respect to the first excited state there is a 15.8 % and 15.1 % increase in the energy splitting for **1-noTHF** and **1-noI** respectively. While the difference between **1-noTHF** and **1-noI** is minimal at the first excited state, in the second excited state the effect of the THF molecules on the electronic structure is greater. Removal of such moieties produces a 22.2 % increase over **1-Dy**, whereas removal of the iodine ligand in **1-noI** only produces a 13.7 % increase over **1-Dy**. This is conceivable as Dy-I bonds are characteristically weak, meaning that its contribution to the total ligand field of the parent compound is less with respect to the oxophilic interaction of Dy^{III} with THF. From this we suspect that the THF molecules are producing a competitive, perpendicular ligand field with that generated by the nitrogen atoms of the NN^{TBS} ligand, which likely contributes to the diminished energy barrier.

When all of the transverse ligands are removed, as in **1-noTHFnoI**, a 33.3 % increase in the energy splitting of the first excited state is observed. In terms of the magnetic structure, this translates well, revealing $g_Z >> g_X, g_Y$ even in the fourth KD. Thus, providing evidence for what would be a near threefold improvement (535.7 cm^{-1} *vs.* 1591.1 cm^{-1}) on the energy barrier to spin reversal for a Dy^{III} SMM with a rigid ferrocene diamide framework. Interestingly, the obtained *g*-tensors for **1-noI** in the fourth KD are less axial in comparison to **1-Dy**, whereas **1-noTHF** and **1-Dy** display similar *g*-tensors. The inferior axiality of **1-noI** once again can be reasoned by the competitive, perpendicular ligand field generated by the remaining THF molecules. Thus, demonstrating the immediate significance of removing or replacing these moieties with weaker-field ligands. Through this systematic study of *g*-tensors combined with the low-lying energy spectra, we are finding ways to improve the local magnetic axiality of molecular species. This leads to the conclusion that future work should be devoted to finding suitable equatorial ligands that do not affect the crystal field splitting of the main lanthanide ion or to avoid equatorial ligands, if possible.[5, 8]

Our study highlights a new design approach towards mimicking the elusive two coordinate Dy^{III}, although the presence of a coordinated solvent and iodide ligand prevent the maximum energy barrier that could theoretically be achieved for such a system (≈1600 cm^{-1} for **1-Dy in the absence of THF and I**). The functionalized ferrocene backbone of the NN^{TBS} ligand offers a truly unparalleled synthetic approach towards harnessing single-ion anisotropy. Through careful synthetic modifications, the contributions of the equatorial/transverse ligands may be altered by replacement with weaker crystal field ligands, effectively allowing for finite tuning of the magnetic axiality. While two coordinate Dy^{III} compounds will undoubtedly remain a synthetic challenge, the use of rigid diamide ligands represents a promising approach for imposing pseudo-axial ligand fields in the development of high temperature lanthanide based SIMs with predictable and defined magnetic axiality.

ASSOCIATED CONTENT

Supporting Information

Supporting Information is available free of charge on the ACS Publications website.
Experimental and computational details (PDF)

AUTHOR INFORMATION

Corresponding Author

*Email: liviu.ungur@chem.kuleuven.be (L. U.)
*Email: pld@chem.ucla.edu (P. L. D.)
*Email: m.murugesu@uottawa.ca (M. M.)

Notes

The authors declare no competing financial interest.

ACKNOWLEDGMENT

The authors gratefully acknowledge the University of Ottawa, the Canadian Foundation for Innovation, and the Natural Sciences and Engineering Research Council Canada, Discovery and RTI grants for their financial support. The synthetic work was supported by the National Science Foundation (Grant 1362999 to PLD). L.U. is a postdoc of the FWO (Fonds Wetenchappelijk Onderzoek – Vlaanderen) and also gratefully acknowledges financial support from Methusalem and INPAC grants from the K. U. Leuven.

REFERENCES

1. Chen, Y.-C.; Liu, J.-L.; Ungur, L.; Liu, J.; Li, Q.-W.; Wang, L.-F.; Ni, Z.-P.; Chibotaru, L. F.; Chen, X.-M.; Tong, M.-L. *J. Am. Chem. Soc.* **2016,** *138*, 2829-2837.
2. Meihaus, K. R.; Long, J. R. *J. Am. Chem. Soc.* **2013,** *135*, 17952-17957.
3. Ungur, L.; Le Roy, J. J.; Korobkov, I.; Murugesu, M.; Chibotaru, L. F. *Angew. Chem. Int. Ed.* **2014,** 53, 4413-4417.
4. Pugh, T.; Tuna, F.; Ungur, L.; Collison, D.; McInnes, E. J. L.; Chibotaru, L. F.; Layfield, R. A. *Nat. Commun.* **2015,** *6*, 7492.
5. Gregson, M.; Chilton, N. F.; Ariciu, A.-M.; Tuna, F.; Crowe, I. F.; Lewis, W.; Blake, A. J.; Collison, D.; McInnes, E. J. L.; Winpenny, R. E. P.; Liddle, S. T., A. *Chem. Sci.* **2016,** *7*, 155-165.
6. Zadrozny, J. M.; Xiao, D. J.; Atanasov, M.; Long, G. J.; Grandjean, F.; Neese, F.; Long, J. R. *Nat. Chem.* **2013,** 5, 577-581.
7. Chilton, N. F. *Inorg. Chem.* **2015,** *54*, 2097-2099.
8. Ungur, L.; Chibotaru, L. F. *Inorg. Chem.* **2016,** DOI: 10.1021/acs.inorgchem.6b01353.
9. Huang, W.; Le Roy, J. J.; Khan, S. I.; Ungur, L.; Murugesu, M.; Diaconescu, P. L. *Inorg. Chem.* **2015,** *54*, 2374-2382.
10. Fortier, S.; Le Roy, J. J.; Chen, C.-H.; Vieru, V.; Murugesu, M.; Chibotaru, L. F.; Mindiola, D. J.; Caulton, K. G. *J. Am. Chem. Soc.* **2013,** *135*, 14670-14678.
11. Guillet, G. L.; Sloane, F. T.; Ermert, D. M.; Calkins, M. W.; Peprah, M. K.; Knowles, E. S.; Čižmár, E.; Abboud, K. A.; Meisel, M. W.; Murray, L. J. *Chem. Commun.* **2013,** *49*, 6635-6637.
12. Alvarez, S.; Llunell, M., *J. Chem. Soc., Dalton Trans.* **2000,** 3288-3303.
13. Zhang, J.; Yi, W.; Chen, Z.; Zhou, X. *Dalton Trans.* **2013,** *42*, 5826-5831.
14. Anfang, S.; Harms, K.; Weller, F.; Borgmeier, O.; Lueken, H.; Schilder, H.; Dehnicke, K. *Z. Anorg. Allg. Chem.* **1998,** *624*, 159-166.
15. Yang, S.; Troyanov, S. I.; Popov, A. A.; Krause, M.; Dunsch, L. *J. Am. Chem. Soc.* **2006,** *128*, 16733-16739.
16. Zhang, P.; Zhang, L.; Wang, C.; Xue, S. F.; Lin, S. Y.; Tang, J. K. *J. Am. Chem. Soc.* **2014,** *136*, 4484-4487.
17. Zhao, L.; Xue, S.; Tang, J. *Inorg. Chem.* **2012,** *51*, 5994-5996.
18. Shannon, R. D. *Acta Cryst. A* **1976,** *32*, 751-767.
19. Rinehart, J. D.; Long, J. R. *Chem. Sci.* **2011,** *2*, 2078-2085.
20. Rinehart, J. D.; Meihaus, K. R.; Long, J. R. *J. Am. Chem. Soc.* **2010,** *132*, 7572-7573.
21. Liu, J.; Chen, Y.-C.; Liu, J.-L.; Vieru, V.; Ungur, L.; Jia, J.-H.; Chibotaru, L. F.; Lan, Y.; Wernsdorfer, W.; Gao, S.; Chen, X.-M.; Tong, M.-L. *J. Am. Chem. Soc.* **2016,** *138*, 5441-5450.
22. Pugh, T.; Chilton, N. F.; Layfield, R. A. *Angew. Chem. Int. Ed.* **2016,** DOI: 10.1002/anie.201604346.
23. Gatteschi, D.; Sessoli, R.; Villian, J. *Molecular Nanomagnets*. Oxford University Press: Oxford, **2006**.
24. Liddle, S. T.; van Slageren, J. *Chem. Soc. Rev.* **2015,** *44*, 6655-6669.
25. Orbach, R. *Proc. R. Soc. London Ser. A* **1961,** *264*, 458-484.
26. Williams, U. J.; Mahoney, B. D.; DeGregorio, P. T.; Carroll, P. J.; Nakamaru-Ogiso, E.; Kikkawa, J. M.; Schelter, E. J. *Chem. Commun.* **2012,** *48*, 5593-5595.
27. Aquilante, F.; Autschbach, J.; Carlson, R. K.; Chibotaru, L. F.; Delcey, M. G.; De Vico, L.; Galvan, I. F.; Ferre, N.; Frutos, L. M.; Gagliardi, L.; Garavelli, M.; Giussani, A.; Hoyer, C. E.; Li Manni, G.; Lischka, H.; Ma, D.; Malmqvist, P. A.; Mueller, T.; Nenov, A.; Olivucci, M.; Pedersen, T. B.; Peng, D.; Plasser, F.; Pritchard, B.; Reiher, M.; Rivalta, I.; Schapiro, I.; Segarra-Marti, J.; Stenrup, M.; Truhlar, D. G.; Ungur, L.; Valentini, A.; Vancoillie, S.; Veryazov, V.; Vysotskiy, V. P.; Weingart, O.; Zapata, F.; Lindh, R., *J. Comput. Chem.* **2016,** *37*, 506-541.
28. Ungur, L.; Chibotaru, L. F. *Phys. Chem. Chem. Phys.* **2011,** *13*, 20086-20090.
29. Ungur, L.; Thewissen, M.; Costes, J.-P.; Wernsdorfer, W.; Chibotaru, L. F. *Inorg. Chem.* **2013,** 52, 6328-6337.
30. Speldrich, M.; Schilder, H.; Lueken, H.; Koegerler, P. *Isr. J. Chem.* **2011,** *51*, 215-227.
31. Baldovi, J. J.; Clemente-Juan, J. M.; Coronado, E.; Gaita-Arino, A. *Inorg. Chem.* **2014,** 53, 11323-11327.

Authors are required to submit a graphic entry for the Table of Contents (TOC) that, in conjunction with the manuscript title, should give the reader a representative idea of one of the following: A key structure, reaction, equation, concept, or theorem, etc., that is discussed in the manuscript. Consult the journal's Instructions for Authors for TOC graphic specifications.

Insert Table of Contents artwork here